Image reconstruction in cross-sectional optoacoustic tomography based on non-negative constrained model-based inversion

Lu Ding, Xose Luís Deán-Ben, Christian Lutzweiler, Daniel Razansky, and Vasilis Ntziachristos*

Institute for Biological and Medical Imaging (IBMI), Helmholtz Zentrum München and Technische Universität München, Ingolstädter Landstraße 1, 85764 Neuherberg, Germany

ABSTRACT

In optoacoustic tomography, images representing the light absorption distribution are reconstructed from the measured acoustic pressure waves at several locations around the imaged sample. Most reconstruction algorithms typically yield negative absorption values due to modelling inaccuracies and imperfect measurement conditions. Those negative optical absorption values have no physical meaning and their presence hinders image quantification and interpretation of biological information. We investigate herein the performance of optimization methods that impose non-negative constraints in model-based optoacoustic inversion. Specifically, we analyze the effects of the non-negative restrictions on image quality and accuracy as compared to the unconstrained approach. An efficient algorithm based on the projected quasi-Newton scheme and the limited-memory Broyden-Fletcher-Goldfarb-Shannon method is used for the non-negative constrained inversion. We showcase that imposing non-negative constraints in model-based reconstruction leads to a quality increase in cross-sectional tomographic optoacoustic images.

Keywords: optoacoustic tomography, photoacoustic tomography, model-based inversion, non-negative constrained least squares

1. INTRODUCTION

Image reconstruction of the optical absorption distribution from the measured pressure signals is an essential step regarding the performance of an optoacoustic tomographic imaging system. Indeed, key factors such as the resolution, quantitativeness and reconstruction time are determined by the accuracy and computational efficiency of the reconstruction algorithm employed.

Analytical back-projection approaches have been extensively utilized for tomographic imaging due to their simplicity and low computational time [1]. However, negative values, quantitative inaccuracies, streak-type artifacts and other errors affect images reconstructed with back-projection approaches. Model-based optoacoustic algorithms have been developed as more accurate alternatives to back-projection methods [2] [3] [4] [5] [6]. In model-based procedures, inversion is done by numerically minimizing the error between the measured signals and those theoretically predicted by a linear optoacoustic forward model. Typically, the corresponding least squares problem is solved without constraints by application of an iterative algorithm such as the LSQR [7].

Model-based methods allow accounting for distorting effects in the forward model. For example, the effects of the detector employed or acoustic heterogeneities in the imaged object can be modeled [3] [8] [9]. Therefore, a forward model can be built that better matches the real experimental situation compared to the idealized assumptions, leading to more accurate inversions. However, even though such complex models generally improve the reconstruction accuracy over back-projection approaches, the forward model may not perfectly

-

Opto-Acoustic Methods and Applications in Biophotonics II, edited by Vasilis Ntziachristos, Roger Zemp, Proc. of SPIE Vol. 9539, 953919 \cdot © 2015 SPIE \cdot CCC code: 1605-7422/15/\$18 \cdot doi: 10.1117/12.2183947

v.ntziachristos@tum.de

account for all experimental parameters. In addition, the tomographic information collected may be incomplete, i.e. the sound waves may only be collected in limited-view angles or with finite-bandwidth ultrasound detectors. Such imperfections result in the appearance of negative values in the reconstructed images. These negative values have no physical meaning since the absorbed optical energy can only be higher or equal than zero, but are introduced during the inversion process as part of the minimization computation. Indeed, the development of a perfect forward model is generally unattainable, so that negative values commonly appear in the reconstructed images. For instance, model-based reconstruction in cross-sectional tomographic imaging systems is typically done by assuming optoacoustic sources confined in a plane [10], which is an approximation considering the three dimensional excited region and the imperfect rejection of out-of-plane signals with cylindrically focused ultrasound transducers. Also, some imaging systems are constrained to detect sound only at certain angular positions, which results in limited-view acquisition further compromising the reconstruction performance and similarly leading to negative value artifacts.

The negative values in the reconstructed images are usually thresholded to zero. A more rigorous approach is to set non-negative restrictions to the inversion problem. Conventionally, numerical inversion is computationally burdensome. As recent imaging systems allow generation of tomographic datasets at video rate, the inversion process has become the bottleneck for accurate fast imaging. Imposing additional constraints further increases the inversion times for large-scale problems in optoacoustic tomography. However, algorithms that are used for unconstrained large-scale optimization problems (e.g. the limited-memory Broyden-Fletcher-Goldfarb-Shannon (LBFGS) method) can be adapted to handle simple box constraints such as the non-negativity constraint.

Herein, we investigate the performance of non-negative constrained model-based inversion and compare the results to those obtained with the unconstraint approach. We use data from imaging experiments with tissue-mimicking phantoms and mice *in vivo*. We observe in our experiments that inversion with an explicit non-negativity constraint leads to results with more information than those obtained in the unconstrained case when the negative values are thresholded to zero.

2. THEORY

Model-based reconstruction

In a two dimensional imaging geometry, the pressure wave that results from the absorption of a laser pulse is modeled as [10] [11]

$$p(r,t) = \frac{\Gamma}{4\pi c} \frac{\partial}{\partial t} \int_{L'(t)} \frac{H(r')}{|r-r'|} dL'(t)$$
 (1)

where Γ is the dimensionless Grueneisen parameter, c is the speed of sound in the medium and H is the amount of energy absorbed in the tissue per unit volume. The integral is performed along a circumference L'(t) with radius |r-r'|=ct. This model is valid as long as the excitation with the laser pulses fulfills the stress and thermal confinement conditions and the speed of sound is uniform within the medium. Furthermore, it is assumed that the optoacoustic sources are confined in the imaging plane (cross-section). The linear relation of the continuous absorption function and the pressure signal in (1) is then discretized and we obtain a linear system of equations [2]

$$p = Ah \tag{2}$$

where p denotes the pressure signals at discrete time instants and h is the vector of optical absorptions sampled in a uniform two-dimensional grid. The model matrix h is the discretization of (1) and depends on the geometry of the experimental setup and the speed of sound in the medium.

For the unconstrained reconstruction, we simply have to minimize the least squared error between the measured pressure signal p_m and the pressure signal predicted by the forward model in (2), i.e. to solve the least-squares problem given by

$$\widehat{h} = \operatorname{argmin}_{h} \| p_{m} - Ah \|_{2}^{2}. \tag{3}$$

Due to the large dimensionality of the problem, the reconstruction is typically done with an iterative method, for example the LSQR algorithm.

Non-negative reconstruction

By introducing non-negativity constraints, image reconstruction is performed by solving the non-negative constrained least squares (NNLS) problem given by

$$\widehat{\boldsymbol{h}} = \operatorname{argmin}_{\boldsymbol{h} \geq \boldsymbol{0}} \|\boldsymbol{p}_m - \boldsymbol{A}\boldsymbol{h}\|_2^2. \tag{4}$$

The problem is convex since the cost function is convex and we have linear constraints. However, a typical convex solver is not applicable due to the high dimensionality of the problem. Methods like LBFGS, which is a reduced memory quasi-Newton method, can be applied to very large, unconstrained problems [12]. Fortunately, the LBFGS method can be extended to the handle the simple non-negativity constraint [13].

3. METHODS

The performance of the non-negative constrained inversion in optoacoustic cross-sectional model-based reconstruction was evaluated with experimental measurements from phantoms and small animals *in-vivo*. The experiments were done with two cross-sectional optoacoustic tomography systems based on signal acquisition with an array of cylindrically focused transducers. The first system consists of 64 transducer elements with 172° angular coverage, while the second system is based on an array of 256 transducers with 270° angular coverage [14].

We first investigated the performance of the NNLS approach in terms of the squared residual. In this experiment, two polyethylene tubings were inserted in the central region of a tissue-mimicking phantom. The tubings contained India ink with different concentrations corresponding to optical absorption coefficients of $\mu_a = 1 \text{cm}^{-1}$ and $\mu_a = 2 \text{cm}^{-1}$. Imaging was done with the 64 element system. The reconstruction performance of the NNLS approach was compared to the unconstrained case, which contains negative artifacts, and to the case with unconstrained reconstruction where all negative values were set to zero.

In a second experiment, we used the 256-element system to obtain cross-section images of mice *in vivo* in the region of kidney and post-mortem in the brain area. We again compared the image quality of NNLS reconstruction with unconstrained reconstruction where negative values were set to zero.

4. RESULTS

Fig. 1 displays the phantom imaging results obtained with the different reconstruction approaches. Fig 1a shows the result of unconstrained reconstruction, which contains negative artifacts in the background and in the interior of the phantom (marked in red). Fig 1b shows the same image with negative values thresholded to zero. Fig 1c illustrates the result of non-negative constrained reconstruction. It is shown that the NNLS approach conserves more of the internal information of the image.

In Fig. 1d the performance of the NNLS approach with respect to the number of iterations of the projected quasi-Newton LBFGS algorithm (PQN-LBFGS) is represented. Each dot in the PQN-LBFGS curve denotes a single iteration. It is shown that the squared error decreases with iterations until the algorithm converges. The squared errors for unconstrained reconstruction and unconstrained reconstruction with thresholding are included for comparison. The squared error of the unconstrained reconstruction without thresholding is obviously lower than that of the NNLS approach since the NNLS approach incorporates an additional constraint. However, we note that a small number of iteration is sufficient for the NNLS approach to outperform the reconstruction when thresholding is performed.

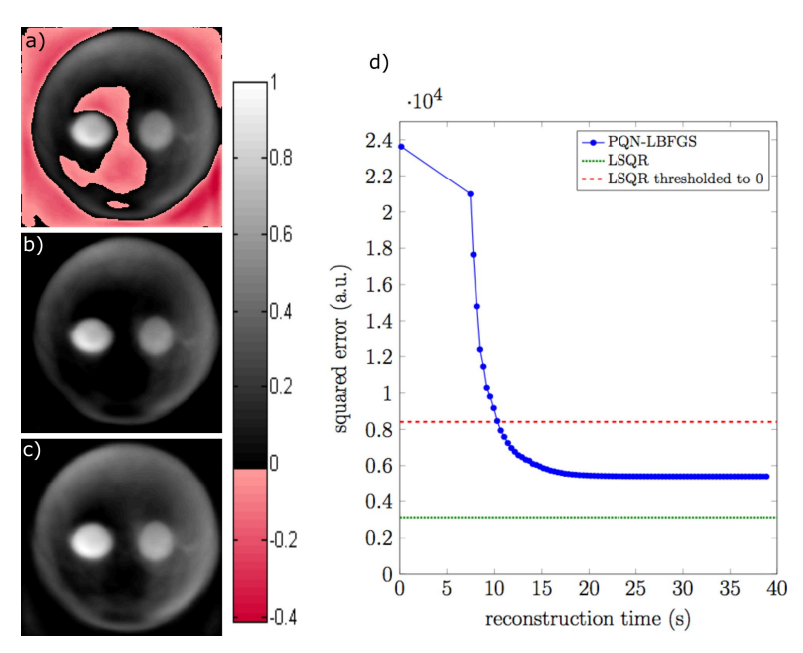


Figure 1. Performance of NNLS compared to standard LSQR reconstructions. (a) Standard unconstrained inversion (LSQR) with negative values shown in red. (b) Same inversion procedure as in (a) with negative values thresholded to zero. (c) NNLS inversion (the PQN-LBFGS method). (d) Squared residual as a function of time and iterations (blue dots) for the NNLS inversion procedure. As a reference, the squared residual obtained after 20 iterations for the unconstrained inversion with and without thresholding negative values to zero are displayed in green and red respectively.

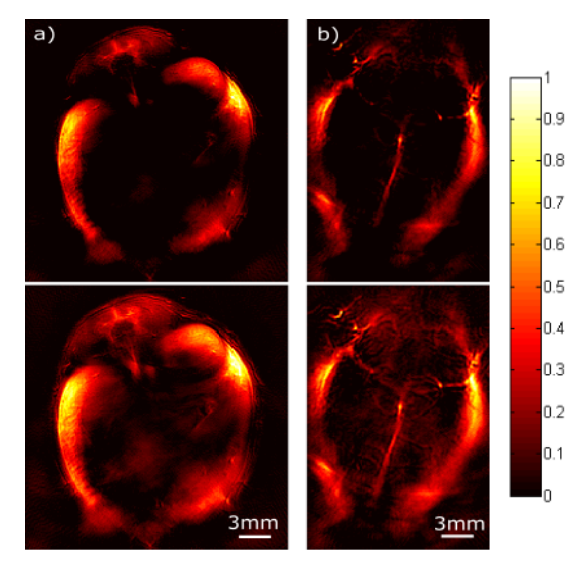


Figure 2. Tomographic reconstructions of two different mice areas, namely the kidney region (a) and the brain region (b). The first row shows the reconstructed images using the standard inversion (LSQR) with negative values thresholded to zero. The second row shows the equivalent reconstructions with the non-negative constrained inversion (the PQN-LBFGS method).

Fig. 2 displays two cross-sectional images of mice, which were taken with the 256-element cross-sectional system. The first row shows the resulting images with the thresholding approach and the second row the equivalent images obtained with NNLS inversion. The loss of structure is observed in the internal area of the image when thresholding is applied. This is due to the low absorption values within the tissue, which are reconstructed as negative artifacts in the unconstrained reconstruction. The NNLS approach, on the contrary, preserves the internal structure of the image without introducing any negative artifacts.

5. CONCLUSION

It was observed in the presented experiments that the NNLS reconstruction leads to a smaller residual as compared to the thresholding approach. Additionally, it was shown that the internal structure of both the phantom and the mouse images are better preserved with the NNLS approach than the thresholded images. Since negative values destroy the physical integrity of the image, the presented results motivate the use of non-negative constrained reconstruction in optoacoustic imaging.

ACKNOWLEDGMENT

D.R. acknowledges support from the European Research Council under grant agreement ERC-2010-StG-260991. V.N. acknowledges support from the European Union project FAMOS (FP7 ICT, Contract 317744).

REFERENCES

- [1] Xu, M. and Wang,L.V., "Universal back-projection algorithm for photoacoustic computed tomography," Physical Review E, 71(1):016706, (2005).
- [2] Dean-Ben, X.L., Buehler, A., Ntziachristos, V. and Razansky. D., "Accurate model-based reconstruction algorithm for three-dimensional optoacoustic tomography," Medical Imaging, IEEE Transactions on, 31(10):1922–1928, (2012).
- [3] Mitsuhashi, K., Wang, K. and Anastasio, M. A., "Investigation of the far-field approximation for modeling a transducer's spatial impulse response in photoacoustic computed tomography," Photoacoustics, 2(1):21–32, (2014).
- [4] Paltauf, G., Viator, J.A., Prahl, S.A., Jacques, S.L., "Iterative reconstruction algorithm for optoacoustic imaging," The Journal of the Acoustical Society of America 112.4 (2002): 1536-1544.
- [5] Dean-Ben, X.L., Ma, R., Rosenthal, A., Ntziachristos, V. and Razansky, D.," Weighted model-based optoacoustic reconstruction in acoustic scattering media," Physics in medicine and biology, 58(16):5555, (2013).
- [6] Christian, L., Deán-Ben, X.L. and Razansky, D., "Expediting model-based optoacoustic reconstructions with tomographic symmetries," Medical physics 41.1 (2014): 013302.
- [7] Paige, C. C. and Saunders, M. A., "LSQR: An Algorithm for Sparse Linear Equations And Sparse Least Squares," ACM Trans. Math. Soft., Vol.8, (1982), pp. 43-71.
- [8] Huang, C., Nie, L., Schoonover, R. W., Wang, L. V. and Anastasio, M.A.," Photoacoustic computed tomography correcting for heterogeneity and attenuation," Journal of biomedical optics, 17(6):0612111–0612115, (2012).
- [9] Rosenthal, A., Ntziachristos, V. and Razansky, D., "Model-based optoacoustic inversion with arbitrary-shape detectors," Medical physics, 38(7):4285–4295, (2011).
- [10] Rosenthal, A., Razansky, D. and Ntziachristos, V., "Fast semi-analytical model-based acoustic inversion for quantitative optoacoustic tomography," Medical Imaging, IEEE Transactions on 29.6 (2010): 1275-1285.

Proc. of SPIE Vol. 9539 953919-5

- [11] Deán-Ben, X. L., Ntziachristos, V. and Razansky, D., "Acceleration of optoacoustic model-based reconstruction using angular image discretization," Medical Imaging, IEEE Transactions on 31.5 (2012): 1154-1162.
- [12] Byrd, R. H., Lu, P., Nocedal, J. and Zhu, C., "A limited memory algorithm for bound constrained optimization," SIAM J. Sci. Comput., 16(5):1190–1208, September (1995).
- [13] Kim, D., Sra, S. and Dhillon, I., "Tackling box-constrained optimization via a new projected quasi-newton approach," SIAM Journal on Scientific Computing, 32(6):3548–3563, (2010).
- [14] Razansky, D., Buehler, A., and Ntziachristos, V., "Volumetric real-time multispectral optoacoustic tomography of biomarkers," Nature protocols, 6(8):1121–1129, (2011).

Proc. of SPIE Vol. 9539 953919-6